A General Framework for Predicting the Temperature-Dependence of Microbial Interactions

Quqiming Duan[1,*], Will Harcombe[2], Van Savage[3], Michael Mustri[4], Thomas P. Smith[1], Samraat Pawar[1,*]

1. Imperial College London, Silwood Park Campus, Ascot, UK; 2. Ecology, Evolution and Behavior, University of Minnesota, Minneapolis, MN, USA 3. Department of Ecology and Evolutionary Biology, University of California Los Angeles, USA 4. University of Arizona, Department of Ecology and Evolutionary Biology, Tucson, Arizona, USA

∗ Corresponding authors; e-mail: d.duan20@imperial.ac.uk, s.pawar@imperial.ac.uk

Abstract

A general mechanistic understanding of the impacts of temperature on resource-mediated interactions between microbial species is currently lacking. Here, we develop a trait-based mathematical framework to derive the temperature-dependence of effective pairwise species interactions within a microbial community that accounts for higher-order interactions. Parameterising this framework using bacterial metabolic traits leads to three key predictions. First, species' effective interactions respond unimodally to environmental temperature and are typically more thermally sensitive than their underlying metabolic processes (e.g., resource uptake and respiration). Second, the temperature response of interactions is mainly governed by resource competition. Third, the mean and variance of intraspecific interaction strengths increase with temperature faster than interspecific interactions. These findings have key implications for our understanding of microbial community dynamics in natural environments, paving the way for predicting the impacts of temperature fluctuations and change on their coexistence, diversity, and stability.

1 Introduction

It is one of nature's most profound facts that no organism exists in isolation. This is especially true for microbes, which in the real world typically exist in complex communities structured by interactions between trillions of cells, thousands of strains, and hundreds of species (Thompson et al. 2017, Machado et al. 2021, The Human Microbiome Project Consortium et al. 2012). The interactions between and within microbial species are particularly crucial because Bacteria, Archaea, Fungi, and Protists collectively dominate heterotrophic biomass in practically all ecosystems (Bar-On et al. 2018) and drive the cycling of energy and matter by consuming and recycling organic matter, as well as limiting nutrients such as nitrogen and phosphorus (Philippot et al. 2013, Handley 2019, Malik et al. 2020). In all of this, prokaryotes, and in particular bacteria, play a dominant role due to their high biomass abundance relative to other microbial groups (Bar-On et al. 2018, Rivett & Bell 2018).

Bacterial cells interact with each other in three ways through resource use (henceforth, "resource-mediated interactions"): competing directly for shared substrates, cross-feeding on each other's metabolic by-products (e.g., facilitation, mutualism), and affecting each other's growth indirectly by modifying the environment (e.g., high-order interactions). At the same

time, key physiological (metabolic) traits—resource uptake and allocation, growth, and maintenance respiration rates, all respond unimodally to temperature (Fig. 1, Schoolfield et al. 1981, Hobbs et al. 2013, Dell et al. 2014, Corkrey et al. 2012, DeLong et al. 2017). Since interactions between microbial species depend on the partitioning and metabolic transformation of resources, environmental temperature also affects the type (e.g. competition versus cooperation) and the strength of interactions between them (Bestion et al. 2018, Kaur & Dutta 2020), which in turn can affect species' metabolic traits (García et al. 2023).

Understanding the temperature dependence of resource-mediated bacterial species interactions is critical for two reasons. First, these interactions determine the rate of collective community functioning (Lechón-Alonso et al. 2021, Pascual-García et al. 2020, Tikhonov 2016). For example, the temperature dependence of the efficiency of community carbon use depends on the nature of species interactions (e.g., balance of competition versus cooperation) (García et al. 2023, Pold et al. 2020). Second, resource-mediated interactions determine microbial community feasibility (possibility of coexistence; Clegg & Pawar 2024) and stability, as well as reactivity (how well the community can withstand perturbations; Barabás et al. 2014). In this context, predicting the relative strengths of inter- and intra-specific interactions (self-regulation) is of particular consequence (Barabás et al. 2017). The importance of the temperature dependence of both these aspects—functioning and feasibility-stability—also means that understanding microbial species interactions is key not only for investigating ecological patterns, but also for the successful engineering of community functions in natural environments (e.g. microbial fertilizers), where environmental temperatures vary both geographically and temporally at scales ranging from daily cycles to global warming (Woolway et al. 2016, Karger et al. 2017, NOAA 2024).

Currently, methods to predict the temperature-dependence of resource-mediated pairwise bacterial (and in general heterotrophic microbial) interactions are lacking. To date, studies have either relied on empirical inferences of pairwise microbial species interactions using community-level co-occurrences over time and space (Cazelles et al. 2016, Barberán et al. 2012), or made assumptions based on the Metabolic Theory of Ecology (MTE) (Clegg & Pawar 2024). The empirical co-occurrence-based approach is severely limited and difficult to generalise because several confounding factors can cause species to co-occur, combined with the paucity of temperature-specific community co-occurrence snapshots (Blanchet et al. 2020). On the other hand, although considerable progress has been made through MTE towards understanding the mechanistic basis of temperature-dependent interactions between eukaryotic organisms (Dell et al. 2014, Bestion et al. 2018), these cannot directly be applied to microbial interactions, which are subject to very different metabolic and biophysical constraints (Stark et al. 2024, DeLong et al. 2010, Kempes et al. 2017).

In this study, we develop a method to mechanistically derive microbial species interactions in the context of resource uptake and metabolite secretion by combining MTE and consumer-resource theory. This approach captures all types of interactions on the spectrum of competition to facilitation as pairwise effects between species based on the state of their shared resource environment. Using extensive trait data on bacteria, we then parameterise this framework to address three key questions: (i) What is the distribution of effective, metabolically constrained intraspecific and interspecific species interactions in randomly assembled communities, and how do they respond to changing temperatures? (ii) What aspects of the underlying consumer-resource dynamics govern the temperature dependence of pairwise interactions in the community? (iii) What is the functional form and thermal sensitivity of the emergent temperature-dependence of the pairwise interactions?

2 Methods

Pairwise microbial species interactions are necessarily dependent on the community-wide consumer-resource dynamics. Therefore, to derive the temperature-dependence of species interactions, we incorporate metabolic constraints in the form of thermal performance curves (TPCs; Fig. 1) of species-level traits into a general consumer-resource model. We then calculate the effective Lotka-Volterra system for this model, which yields the temperature dependence of pairwise interactions arising from the underlying (metabolically constrained) consumer-resource dynamics.

2.1 The Consumer-Resource Model

We use a general consumer-resource model based on MacArthur's seminal work (MacArthur 1970, Goldford et al. 2018, Marsland III et al. 2020) (the "Microbial Consumer-Resource Model", aka MiCRM) which tracks biomass fluxes and dynamics in the community by explicitly accounting for resource uptake, metabolic by-product secretion and cross-feeding, and maintenance respiration. Species within the community compete through the exploitation of resources and cross-feed through secretion of metabolic by-products, which replenish the resource pool. For a community of N species (or "strains") and M resource types, the MiCRM is:

$$\frac{dC_i}{dt} = C_i \left(\sum_a u_{ia}(T)(1 - \sum_b l^i_{ab}) R_a - m_i(T) \right), \tag{1}$$

$$\frac{dR_a}{dt} = \rho_a(R) - \sum_{i=1}^{N} \Big(C_i u_{ia}(T) R_a - \sum_{b=1}^{M} C_i u_{ib}(T) R_b l^i_{ba} \Big). \tag{2}$$

Here, C_i $(i = 1, ..., N)$ is the biomass abundance of the ith consumer species and R_a $(a = 1, ..., M)$ the resource abundance of the ath resource type. All resource types are generated externally and enter the system at a constant rate (ρ_a). The ith population's growth is determined by its (temperature-, T-dependent) resource uptake $(u_i(T))$ and loss rate (to maintenance respiration, $m_i(T)$). The total uptake rate of the ith species, u_i, is determined by its vector of resource preferences (of u_{ia}'s; Fig. 1). The total resource consumed by each species is lost through inefficiency (l^i_{aa}) or transformation into metabolic by-products (l^i_{ab}) and returned to the resource pool. Assimilation efficiency is bounded at both resource $(1 - \sum_{ib} l^i_{ab} > 0)$ and species $(1 - \sum_{ab} l^i_{ab} > 0)$ levels. Table SI.1 lists and describes all parameters along with their initial values and units.

2.2 Effective species interactions

To study the temperature response of species interactions — while accounting for all indirect and higher-order interactions through resource mediation within microbial communities — we derive an effective Lotka-Volterra (ELV) model from our consumer-resource dynamics. The effective pairwise species interactions are the coefficients of the effective LV (ELV) system of the MiCRM (MacArthur 1970, Marsland et al. 2020), where the ELV is as follows:

$$\frac{dC_i}{dt} \approx C_i (r_i(T) + \sum_j \alpha_{ij}(T) C_j), \tag{3}$$

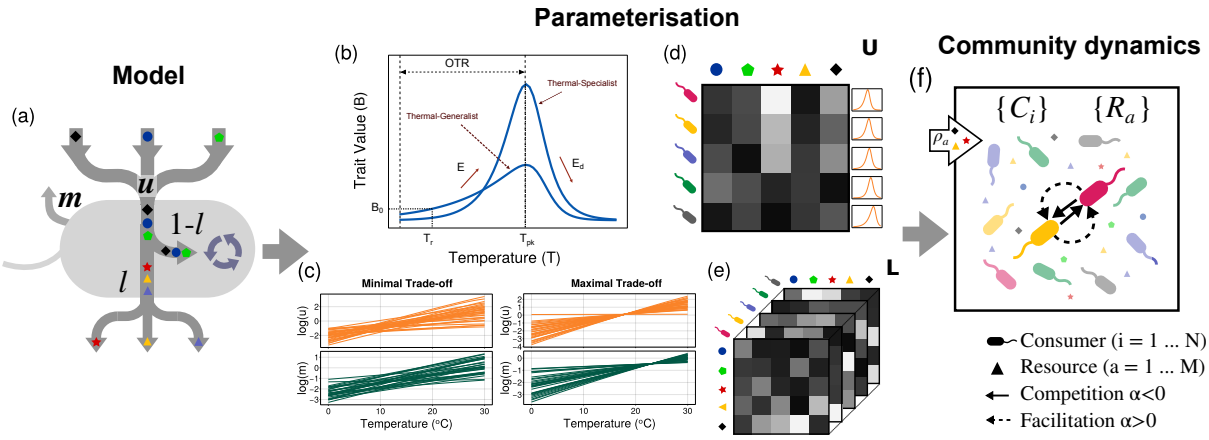

Figure 1: **Schematic of the Microbial Community Model (MiCRM) structure and parameterisation.** (a) Schematic of intracellular metabolic fluxes. Microbial cells uptake resources at rate u, "leak" a proportion (l) of the substrates they uptake as metabolic by-products, using the remaining (1–l) to grow. A portion of the consumed resources is lost to maintenance costs m. (b) Temperature performance curves (TPCs) of metabolic traits—uptake rate u and maintenance cost m—following Eqns. 7 and 8. B_0 denotes the metabolic trait value at a relatively low reference temperature (T_r). These trait values increase exponentially with temperature following the activation energy E, and decline after reaching its peak at T_{pk} due to deactivation, governed by apparent deactivation energy E_d. We consider two thermal strategies: thermal generalists, who perform relatively equally across a broad temperature range, and thermal specialists, who perform better in a narrow optimal temperature range but poorly outside this range. Here we are considering temperatures within the operational temperature range (the temperature range where organisms normally operate, OTR) for most species. (c) TPCs (logged) of metabolic traits with thermal generalist-specialist tradeoff. In the minimal trade-off scenario (correlation coefficient between $\ln(B_0)$ and E is 0), thermal specialists and thermal generalists equally coexist in the initial community. In the maximal trade-off scenario (correlation coefficient between $\ln(B_0)$ and E is -1), the initial community is predominantly composed of thermal specialists. (d) Uptake preference matrix $\mathbf{U}$ of size $N \times M$. The $\mathbf{U}$ matrix consists of the N species' uptake rate vectors of M resource types, representing species-level variation in core metabolic capabilities. (e) Leakage-transformation tensor $\mathbf{L}$. Each strain's metabolic network, encoded in $\mathbf{L}$, determines how consumed substrates are leaked or metabolically transformed. The diagonal elements l^i_{aa} represent the fraction of resource lost through inefficiencies (resource loss), while the off-diagonal elements $l^i_{a\neq b}$ represent secretion of metabolic by-products returned to the resource pool. (f) The dynamics of consumer (C) and resource (R) abundance within the community. The system is initialized with N microbial species and M resource types, with external resources supplied at rate ρ. Microbial species within the community compete for available resources while simultaneously producing metabolic by-products, which can facilitate the growth of other species in the community.

here, r_i and α_{ij} are both implicitly temperature-dependent (denoted by T). The effective interaction and growth rate coefficients can be shown to be (detailed derivation in Sec.SI.1):

$$\alpha_{ij} = \sum_a u_{ia}(1 - l^i_a)\frac{\partial \hat{R}_a}{\partial C_j} \tag{4}$$

$$r_i = \sum_a u_{ia}(1 - l^i_a)\hat{R}_a - \sum_j \alpha_{ij}\hat{C}_j - m_i. \tag{5}$$

The effective interaction matrix is denoted as $\mathbf{A}$:

$$\mathbf{A} = \begin{bmatrix} \sum_a u_{1a}(1-l_a^1)\frac{\partial \hat{R}_a}{\partial C_1} & \dots & \sum_a u_{1a}(1-l_a^1)\frac{\partial \hat{R}_a}{\partial C_N} \\ \vdots & \ddots & \vdots \\ \sum_a u_{Na}(1-l_a^N)\frac{\partial \hat{R}_a}{\partial C_1} & \dots & \sum_a u_{Na}(1-l_a^N)\frac{\partial \hat{R}_a}{\partial C_N} \end{bmatrix} \tag{6}$$

Thus, each effective microbial species interaction embodies the complex manipulation of available resources by different species, including the metabolic transformation and leakage by all species within the community (because the stoichiometric matrix of each species is fully connected; Fig. 1), modulated by the abundance of both consumers and resources at resource equilibrium. Specifically: (i) The impact of species j on i is determined by changes in resource abundances as the former's population grows ($\frac{\partial \hat{R}_a}{\partial C_j}$), mediated by the preferential resource uptake rate of species i (u_{ia}). (ii) Higher-order interactions contribute to these changes in resource abundance since resource uptake rates of all species are incorporated in $\frac{\partial \hat{R}_a}{\partial C_j} = \sum_{bc} D_{ab}^{-1} L_{cb}^j u_{jc} \hat{R}_c$, where $D_{ab} = \frac{\partial \rho_a}{\partial \hat{R}_b} - \sum_i L_{ba}^i C_i u_{ib}$ (Sec.SI.1). (iii) The impact of a species on itself α_{ii} as such has a similar functional form with $\alpha_{i \neq j}$, which is the net effects of competition and cross-feeding from all species in the community. (iv) The ith species' maximal growth rate r_i (its growth rate when species' abundances are low and resources effectively unlimited) is its net assimilation of resources accounting for effects of resource-mediated pairwise interactions minus the (density-independent) maintenance costs: $\sum_a u_{ia}(1-l_a)\hat{R}_a - m_i$.

2.3 Adding Thermal Metabolic Constraints

Species metabolic rates typically display unimodal shapes with temperature (Kontopoulos, van Sebille, Lange, Yvon-Durocher, Barraclough & Pawar 2020, Angilletta Jr & Angilletta 2009), which increase exponentially toward their thermal optimum followed by an exponential decrease due to high-temperature effects. These are normally depicted as temperature performance curves (TPCs, see the Parameterisation section in Fig. 1). We use the modified Sharpe-Schoolfield equation (Kontopoulos, van Sebille, Lange, Yvon-Durocher, Barraclough & Pawar 2020) to model the TPCs of the two species' metabolic traits (Fig. 1):

$$u(T) = \frac{B_{u,0} \times e^{\frac{-E_u}{k}\cdot\left(\frac{1}{T}-\frac{1}{T_r}\right)}}{1 + \frac{E_u}{E_{u,d}-E_u} e^{\frac{E_{u,d}}{k}\cdot\left(\frac{1}{T_{u,pk}}-\frac{1}{T}\right)}} \tag{7}$$

$$m(T) = \frac{B_{m,0} \times e^{\frac{-E_m}{k}\cdot\left(\frac{1}{T}-\frac{1}{T_r}\right)}}{1 + \frac{E_m}{E_{m,d}-E_m} e^{\frac{E_{m,d}}{k}\cdot\left(\frac{1}{T_{m,pk}}-\frac{1}{T}\right)}} \tag{8}$$

Here, each B_0 is a trait-specific normalisation constant; the trait value at a biologically meaningful reference temperature (T_r), which lies within the operational temperature range. Each E is the trait-specific apparent activation energy, which emerges from the convolution of activation energies of the underlying cellular enzymes. As the temperature increases, the metabolic trait increases exponentially following the rate E (which is the activation energy of typically responsible enzyme reactions) until their optimum performance temperature, then the acceleration drops as enzymes begin to deactivate at higher temperatures and the trait value reaches its highest performance at T_{pk}. As the temperature continues to increase and exceeds T_{pk}, the value of metabolic traits decreases exponentially following the rate E_d, which is the apparent deactivation energy. The definitions, initial values and units of all TPC parameters are provided in Table SI.2.

2.4 Assembly Simulations

To calculate the emergent temperature response of effective species interactions, heterotrophic bacterial communities were assembled at different temperatures by random immigration from a global species pool consisting of species with varying TPCs of resource uptake and maintenance respiration rates. The assembly dynamics were simulated according to Eqns 1 - 2 with a random pool of 100 species competing for 50 carbon resources. Example simulation results are shown in SI (Fig.SI.3).

Each species' resource uptake rate (u_i) was subdivided randomly across all M resources (the u_{ia}'s) by sampling resource uptake preferences (proportions) from a Dirichlet distribution (Fig. 1). The leakage-transformation tensor (l^i_{ab}), where metabolic interactions determining leakage and the transformation of consumed resources are different for each species, was also sampled from a Dirichlet distribution such that the sum of the inefficiency of species-level resource utilization on each resource (l^i_a) was 0.3 (Fig. 1).

The assembly simulations were replicated 999 times at each temperature ranging from 0 to 30 °C. All simulation code was written in the Julia language (Bezanson et al. 2017).

2.5 TPC parameterisations

Each species in the immigration pool was assigned randomly generated TPCs for the two traits (u and m; Eqn. 7 and 8). For this, we sampled each species-specific B_0 and E pair (for each of the two traits) from a multivariate normal distribution:

$$\begin{bmatrix} \ln(B_0) \\ E \end{bmatrix} \sim \mathcal{N}(\vec{\mu}, \mathbf{\Sigma}), \tag{9}$$

where, (10)

$$\vec{\mu} = \begin{bmatrix} \mu_{\ln(B_0)} \\ \mu_E \end{bmatrix}, \mathbf{\Sigma} = \begin{bmatrix} \sigma^2_{\ln(B_0)} & \rho_{\ln(B_0),E} \\ \rho_{\ln(B_0),E} & \sigma^2_E \end{bmatrix}, \tag{11}$$

The parameter values were set to: $\overline{E_u} = 0.8146$ eV, $\overline{E_m} = 0.5741$ eV, and $\sigma^2_{\ln(B_{u,0})} = \sigma^2_{\ln(B_{m,0})} = 0.17$ and $\sigma^2_{E_u} = \sigma^2_{E_m} = 0.14$. The correlation coefficient $\rho_{\ln(B_0),E}$, which encodes a thermal generalist-specialist trade-off (see below), was also assumed to be identical for the two traits. The results presented later in this paper are mainly determined by the distribution of the uptake rate as suggested in eqn. 6.

These TPC parameterizations are based on general empirical patterns in data on 604 TPCs for growth rate and metabolic fluxes representative of the bacterial tree of life (Smith et al. 2019, 2021). We refitted these TPC data to the Sharpe-Schoolfield equation using non-linear least squares fitting with the `rTPC` package in R (Padfield et al. 2021). We chose 10°C as the reference temperature (T_r) to avoid extrapolation error, as very few species in the original data are true psychrophiles (extremely cold tolerant) due to experimental constraints. With this T_r, consistent with empirical patterns (Smith et al. 2021), $\overline{T_{pk}}$ for uptake rates ($\overline{T_{p_u}}$) were randomly sampled from a normal distribution such that the $\overline{T_{pk}}$ for respiration rate ($\overline{T_{p_m}}$) of a given species was always higher than that of uptake, ($\overline{T_{p_u}} = 37.98$ and $\overline{T_{p_m}} = 40.60^o$C).

Because empirical data on the TPCs of resource uptake rates in bacteria (and indeed microbes in general) are largely absent, we assumed that the distribution of uptake rate thermal sensitivities (E_u's) is identical to that of maximal growth rates (r_{max}'s). That is, we used the mean and variance of the E distribution of species' r_{max}s as a proxy for $\overline{E_u}$ and $\sigma^2_{E_u}$ (see below). This is based on the assumption that the anabolic processes (e.g., protein synthesis) underlying bacterial r_{max} are mainly constrained by resource uptake (Kempes et al. 2012, 2017). Note that r_{max} here refers to the exponential growth phase of species incubated in isolation, which differs

fundamentally from r_i derived from our ELV. As shown in Eqn.SI.9, r_i additionally incorporates the resource mediation of all interacting species.

This normalisation constant $\overline{B_{0,u}}$ was parameterised by constraining its values to the median value of CUE at T_r (Smith et al. 2021), where:

$$B_{0,CUE} = \frac{\overline{B_{0,u}}(1-l) - \overline{B_{0,m}}}{\overline{B_{0,u}}} = 0.2.$$

Because B_0 follows a log-normal distribution (Fig.SI.2), $\overline{\ln(B_{0,u})} = -0.8116$ and $\overline{\ln(B_{0,m})} = -1.4954$. This constraint ensures the realism of generated species, where species' respiration rates cannot exceed their resource uptake rates, guaranteeing that sufficient resources are transformed into biomass to support species' basic growth.

2.5.1 Thermal generalist-specialist tradeoff as an additional metabolic constraint

In ectotherms, acclimatization or adaptation to one environmental temperature generally comes at the cost of performance at another (Mongold et al. 1996, Angilletta Jr et al. 2002, Ketola & Saarinen 2015). Therefore, TPCs of performance traits (such as u and m) across ectotherms, including microbes, typically exhibit a (thermal) generalist-specialist trade-off (Fig. 1b). That is, TPCs of thermal generalists show moderate levels of performance across a wide range of temperatures, but do not achieve exceptionally high performance at any specific temperature, while those of thermal specialists show high performance within a narrow temperature range but exhibit steep declines in performance outside this range (Huey & Hertz 1984, Gilchrist 1995). By fixing the reference temperature T_r at the lower end of the operational temperature range, this thermal generalist-specialist trade-off can be quantified as a negative correlation between activation energy E and normalisation constant B_0 ($\rho_{\ln(B_0),E}$; Fig. 1 c; Eqn. 9; (Kontopoulos, van Sebille, Lange, Yvon-Durocher, Barraclough & Pawar 2020, Kontopoulos, Smith, Barraclough & Pawar 2020)).

We assume that in any local community assembly dynamic, the value of the thermal generalist-specialist tradeoff $\rho_{\ln(B_0),E}$ varies across species that encounter each other. That is, both thermal generalists and specialists are expected to encounter each other in a local environment (or patch), for two reasons. First, those different species will have inherent differences in the strength of their trade-off ($\rho_{\ln(B_0),E}$) due to differences in their metabolic architecture (e.g., they may represent different phylogenetic groups or metabolic strategies; (Smith et al. 2019, Kontopoulos, Smith, Barraclough & Pawar 2020)). Second, different species in a local environment will likely have adapted to different ecological contexts, especially if the immigration pool covers a larger geographical area. Moreover, the generation times of species within any microbial local assemblage vary across orders of magnitude (from minutes to months or longer) (Gibson et al. 2018), and therefore they experience and adapt to effectively different regimes of environmental temperature fluctuations (Gilchrist 1995, Kontopoulos, van Sebille, Lange, Yvon-Durocher, Barraclough & Pawar 2020).

Therefore, when simulating interactions between species, we consider two extreme cases of the thermal generalist-specialist trade-off distribution (minimal and maximal trade-off levels), with realistic scenarios expected to lie somewhere in between (Fig. 1c). In the minimal trade-off scenario ($\rho_{\ln(B_0),E} \approx 0$), both thermal generalists and specialists exist equally in a local patch. For example, this scenario may arise when the geographical region from which the local community is assembled is large enough so that the species are drawn from multiple different thermal environments. Alternatively, it may arise when the variation in generation times is sufficiently high, allowing species to experience and adapt to frequent thermal fluctuations in their local environments (e.g., in higher-latitude regions). In a maximal trade-off scenario

($\rho_{\ln(B_0),E} \approx -1$), all species are thermal specialists. This scenario would arise when all species are preadapted to a constant environment with no thermal fluctuations, and have no intrinsic variation in the trade-off. Clearly, neither of these extreme scenarios is realistic. For example, even at lower geographical latitudes (the tropics), microbes do experience thermal fluctuations at different timescales.

Finally, note that we assume that the value of $\rho_{B_0,E}$ is the same for u and m. This is based on the fact that current empirical evidence, albeit limited, does not suggest any systematic difference in the correlation between these parameters across microbial trait types (Kontopoulos, Smith, Barraclough & Pawar 2020).

As we further demonstrate in our results, this trade-off plays a crucial role in determining the shape of the temperature performance curves (TPCs) of species interactions.

2.6 Quantifying the the TPCs of effective interactions

To analyse the thermal sensitivities and peak performance temperatures of effective species interactions, we fitted the effective interaction coefficients (α) to the modified Sharpe-Schoolfield model (Kontopoulos, van Sebille, Lange, Yvon-Durocher, Barraclough & Pawar 2020):

$$\alpha(T) = \frac{B_{\alpha,0} \times e^{\frac{-E_\alpha}{k}\cdot\left(\frac{1}{T}-\frac{1}{T_r}\right)}}{1 + \frac{E_\alpha}{E_{\alpha,d}-E_\alpha} e^{\frac{E_{\alpha,d}}{k}\cdot\left(\frac{1}{T_{\alpha,pk}}-\frac{1}{T}\right)}} \tag{12}$$

Non-linear least squares fitting was performed using `curve_fit` from the `LsqFit` package in Julia.

3 Results

3.1 Temperature Systematically Shifts the Distributions of Effective Pairwise Interactions

Fig. 2 shows that effective net interactions within the community are typically negative. Only $\sim 0.002\%$ weakly positive net interactions were observed within all interaction coefficients across the simulated communities. That is, through a combination of competition and facilitation, the effective pairwise species interactions within the communities tend to be net competitive. As temperature increases, the resource uptake rates of species increase exponentially. Therefore, the effective interaction generally becomes more competitive following Eqn. 4 (Fig. 2). On average, intraspecific interactions (α_{ii}) increase in strength with temperature disproportionately faster than interspecific interactions ($\alpha_{i\neq j}$). This is primarily due to the differing emergent distributions of the apparent activation energies for inter- and intraspecific interactions, as explained in the SI (Sec.SI.2). These emergent distributions (of both intraspecific and interspecific interactions) are typically log-normal (Fig. 2), arising from the convolution of the normalization constants of all species' uptake rates within the community. The variance of the interaction distributions is always minimized at intermediate temperature. In addition, there is no correlation between pairwise interactions within the community (between each pair of $\alpha_{i>j}$ and $\alpha_{j>i}$, Fig.SI.4), which has important implications for community feasibility and stability.

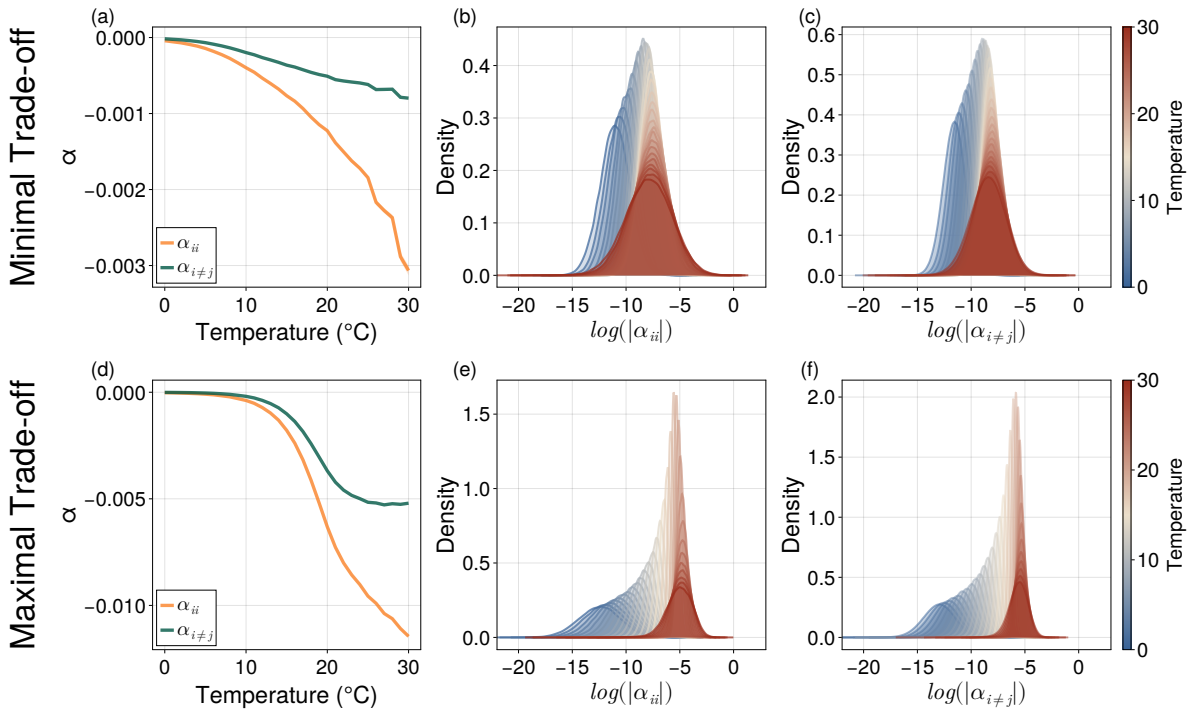

Figure 2: **The effect of temperature on effective, pairwise interaction strengths among bacteria.** (a,d) On average (± SE), intraspecific interactions increase in strength with temperature disproportionately faster than interspecific interactions. The mean values of α_{ii} and $\alpha_{i\neq j}$ at each temperature are calculated from the diagonal and off-diagonal elements of the interaction matrix (**A**, Eqn. 6), respectively, across all simulations. (b,c,e,f) The distributions of both intra- and interspecific interactions are log-normal when metabolically constrained. Mean absolute interaction strengths increases monotonically with temperature, while variance is minimised at intermediate temperatures. These results are from 999 community simulations at each temperature for minimal (a-c, $\rho \approx 0.0$) to maximal (d-f, $\rho \approx -1.0$) thermal generalist-specialist trade-off.

3.2 Effective Competition Dominates the Temperature Response of Interactions

Fig. 3 shows that the response of effective species interactions to changing temperature is driven primarily by competition for limited resource availability. The relative competitive coefficient $\alpha_{j\neq i;j=1,...,N}/\alpha_{ii}$ (for $j = 1, ..., N$) quantifies the relative effects of species i on species j compared to its self-regulation, where $\alpha_{j\neq i;j=1,...,N}$ here denotes all elements in the column of i (when $j \neq i$) in the interaction matrix (**A**, Eqn. 6). This quantity changes unimodally with temperature irrespective of the thermal generalist-specialist trade-off due to changes in species' relative competitive abilities in response to changes in equilibrium resource abundances (Fig. 3). The antagonism among species is always minimized at intermediate temperatures (Sec.SI.2), where equilibrium resource abundance is the highest.

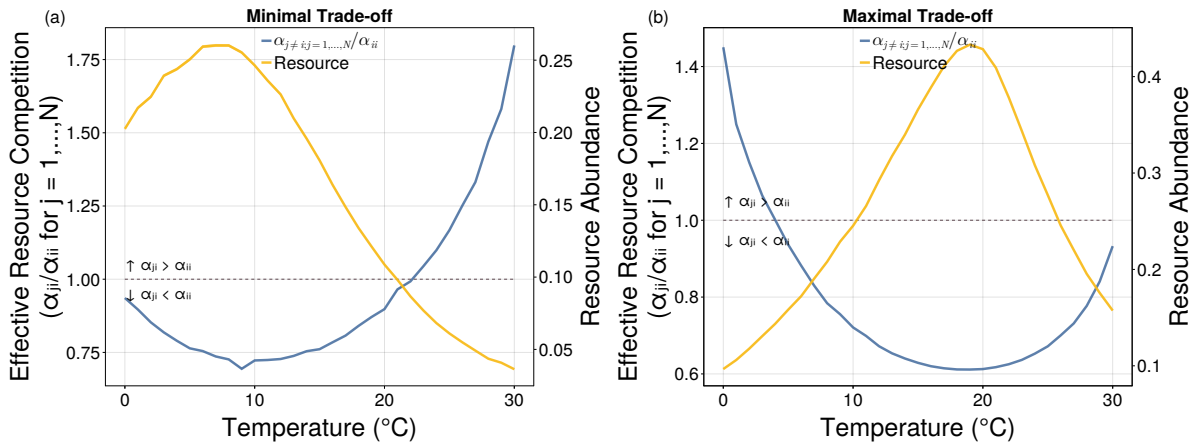

Figure 3: **The thermal responses of species' relative competitiveness ($\alpha_{j\neq i;j=1,\ldots,N}/\alpha_{ii}$).** Mean resource availability (±SE) (yellow line) decreases away from an intermediate temperature (determined by the degree of thermal generalist-specialist tradeoff), where species maximize effective interspecific resource competition (blue line). Dotted line depicts $\alpha_{j\neq i;j=1,\ldots,N}/\alpha_{ii} = 1$. These data are from the same simulations as Fig. 2.

3.3 Interactions are more Thermally Sensitive than Underlying Metabolic Traits

Fig. 4 (and SI Fig.SI.10 - Fig.SI.13) shows that when metabolically constrained, the emergent Temperature Performance Curves (TPCs) of effective species interactions are typically monotonic rising or unimodal, the latter especially when species in the immigration pool exhibit a stronger thermal generalist-specialist trade-off on average (Fig. 1). This arises from the fact that when B_0 and E are negatively correlated, resource exploitation rates at higher temperatures are more strongly bounded, thereby resulting in a monotonic decline in the effective interaction beyond a certain temperature.

The TPCs of intraspecific interactions (α_{ii}s) do not differ in their functional form from those of interspecies interactions ($\alpha_{i\neq j}$) as both are described by similar functions (Eqn. 6). However, intraspecific interactions only have a higher normalization constant on average, again, especially when the generalist-specialist tradeoff is stronger ($B_{0,\alpha}$, Fig.SI.5, which explains why intraspecific interaction strengths increase faster than interspecific ones (Fig. 2).

Effective interactions within the community typically exhibit higher apparent activation energies and relatively lower peak performance temperatures than the underlying metabolic traits, which are uptake and maintenance respiration rates (Fig. 4). We observed median apparent activation energies of $E_\alpha = 1.26$ eV for the community without a thermal generalist-specialist trade-off and 2.07 eV for the community with a strong trade-off. The median peak performance temperatures are $T_{p_\alpha} = 32.64$ and 23.30 °C, respectively. Although the median value appears higher in the first community (Fig. 4 c), there is a secondary peak occurring far below this median value, indicating that peak performance temperatures are generally lower than this median. Most T_{pk} of the effective interactions fall within the operational temperature range of the species. This combination of relatively higher apparent activation energies and relatively lower peak performance temperatures means that effective species interactions are expected to be more sensitive to increasing temperatures, and performances drop at lower temperatures than in the case of underlying metabolic traits.

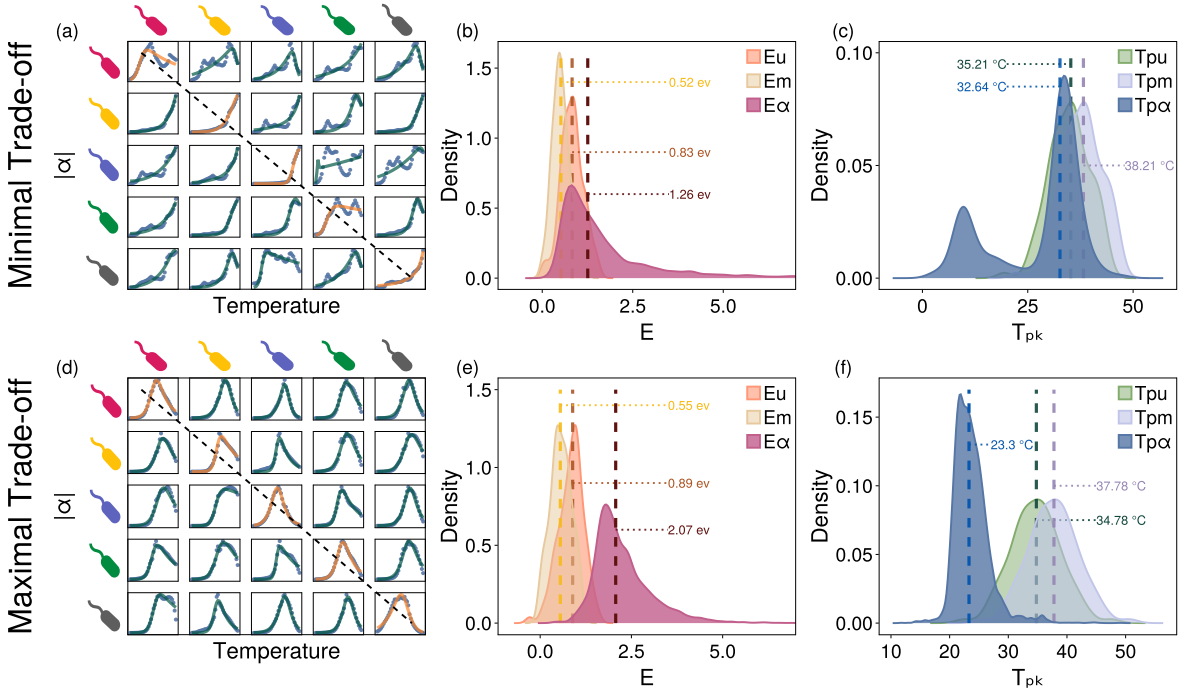

Figure 4: **The temperature performance curves (TPCs) of effective interactions.** (a,d) Representative TPCs of intra- and interspecific interaction coefficients(sub-sample of the coefficients of one of the 100-species communities simulated in Fig. 2). Orange curves depicts the example TPCs of intraspecific interactions (α_{ii}) and green curves depicts the example TPCs of their corresponding interspecific interactions ($\alpha_{i\neq j}$). (b, e) Apparent activation energies of effective interactions (E_α) are typically higher than those of uptake (E_u) and maintenance respiration (E_m) rates. (c, f) The thermal maxima (T_{pk}'s) of interactions (T_{p_α}) are typically lower than that of uptake (T_{p_u}) and maintenance respiration (T_{p_m}) rates. The dotted lines mark median values of distributions.

4 Discussion

We have developed a framework for calculating the temperature dependence of effective pairwise interactions by deriving the effective Lotka-Volterra model from consumer-resource dynamics. Using this framework, we investigated the emergent temperature dependencies of effective species interactions and their dependence on the temperature performance (TPCs) of underlying metabolic traits and the resource dynamics within the system. Our results provide a basis for more precisely predicting how species interactions, and effective resource competition (Fig. 3), drive species sorting (Lee et al. 2023), and thus species richness patterns along temperature gradients.

Previous mechanistic approaches for microbial system dynamics based on the metabolic theory of ecology (MTE) have focused on certain assumed structures of competition and facilitation (Bestion et al. 2018, Clegg & Pawar 2024). These have not accounted for the intercorrelation between species and resource dynamics (Gilbert et al. 2014). Furthermore, these do not consider the potential differences between competitive and facilitative interactions within communities, and the "apparent" activation energy of pairwise bacterial species interactions remains largely unknown empirically and theoretically. For example, Clegg & Pawar (2024) recently assumed

that the temperature dependence of pairwise bacterial species interactions in the generalised Lotka-Volterra (GLV) model follows an Arrhenius response with an activation energy of 1.0 eV on average. However, there is no direct empirical evidence nor mechanistic theory to predict or infer what the actual TPC of inter- and intraspecific species interactions should be. In addition, the mechanistic theory for predicting temperature-dependent species interactions based on multicellular eukaryotes (Dell et al. 2014) cannot straightforwardly be extrapolated to microbes. This is due to several fundamental differences in the biophysical constraints and interactions between uni- and multicells (Kempes et al. 2012, DeLong et al. 2010, Andersen et al. 2016), including respiratory systems, surface area, and resource transportation. In addition, multicellular organisms possess higher levels of functional organisation (e.g., tissues, organs) and more complicated behaviours (e.g., different measures for reproduction).

To study the temperature response of effective microbial species interactions, we parameterised our theory using bacterial TPCs. The results show that for bacteria in particular, the apparent activation energy of pairwise interactions (E_α) lies between $\sim$ 1.26 - 2.07 eV. These values are much higher than the activation energies of species' resource uptake rates and maintenance respiration rates (Fig. 4). This is because species' populations typically require higher energy for resource competition relative to their basic metabolic processes. In addition, while this is an avenue for future work, this high thermal sensitivity of species interactions, not just in terms of their apparent activation energy but also their lower peak performance temperatures (T_{pk}) (Fig. 4), may mean that changes in community dynamics with temperature are primarily driven by changes in competitive abilities rather than direct temperature effects on species-level metabolic traits. Therefore, with environmental (e.g., climatic) warming, species extinctions are more likely than what would have been predicted from considering the TPCs of underlying metabolic traits alone.

Here we parameterised species TPCs using two extreme trade-offs between the activation energies (E) and normalization constants (B_0) of metabolic traits, representing communities from distinct geological origins. As described in Methods, the minimal trade-off scenario best represents microbial communities in higher-latitude (cooler) regions, while the maximal trade-off scenario best represents communities in tropical (hotter) regions. This is supported by the finding that resource competition is minimized at lower temperatures in minimal trade-off communities compared to maximal trade-off communities (Fig. 3), where species tend to evolve to be less antagonistic and more facilitative during co-evolution (Morris et al. 2012, Morris 2015), while adapting to their local thermal environment. In addition, we found that in maximal trade-off communities, activation energies are higher and peak performance temperatures are lower for species interactions relative to minimal trade-off communities, indicating that species interactions in maximal trade-off communities are more thermally sensitive. This suggests that microbial interaction networks in tropical areas may be relatively more susceptible to warming.

The distribution of the normalisation constant B_0 of uptake and respiration rate to the TPC of effective interactions (Fig.SI.5) also has implications for the effects of cell size on species interactions and their consequences for community dynamics. It is well established that each trait-specific normalisation constant B_0 scales with cell mass (M) as

$$B_0 = B_0' M^\theta, \tag{13}$$

where B_0' is a size- and temperature-independent constant, M is cell mass, and θ is an exponent that is broadly consistent within major microbial groups (DeLong et al. 2010, Kempes et al. 2012). Thus, B_0' embodies variation in maintenance metabolic rate across species and strains stemming from differences in metabolic architecture (independent of scaling or thermal constraints), such as surface areas and energy distribution networks, which itself may arise from adaptation or phenotypic plasticity (Gillooly et al. 2001, West et al. 1997). The scaling law

(Eqn. 13) encodes a metabolic constraint stemming from cell size, in addition to the primary focus of this study (temperature). The log-normality of the distribution of normalisation constant B_0 arises from underlying multiplicative processes. In the case of biological systems, and in particular metabolic scaling of cellular processes, cell size distributions within populations are log-normal because the population grows through the (multiplicative) process of cell division (Jafarpour et al. 2018, Jafarpour 2019, Hein & Jafarpour 2024). The corresponding distribution of metabolic rates (and all emergent rates) is log-normal because metabolic processes are essentially the product of multiple factors (a convolution of metabolic, i.e., biochemical pathways). Because we generate our TPC parameterisations by sampling trait spaces derived from experimentally-measured bacterial TPCs, the scaling constraint of cell size is implicitly included in the emergent TPCs of effective interactions. In other words, the log-normality of the distribution of normalisation constant B_0 includes the interspecific cell-size distribution in the underlying TPC datasets.

Since species within a community interact by utilising resources in the environment, different resource abundances are expected to emerge based on their metabolic traits, and in particular, their uptake rates. These regulatory changes in resource abundance are often overlooked in traditional generalised LV models, which do not account for the dynamics of resource abundances. We have shown that equilibrium resource abundance correlates with the ratio of $\alpha_{j\neq i;j=1,\ldots,N}$ and α_{ii} (Fig. 3), a key metric of relative competitiveness between species pairs (Chesson 2000). This ratio quantifies to what extent a given species i can successfully exclude species j; with the possibility of exclusion negatively related to the ratio (when the i species has a greater negative impact on itself than on j). In combination with the result in Fig. 2, we suggest that even with the common existence of facilitative activities (Kehe et al. 2021) such as cross-feeding, effective interactions are typically net competitive towards shared resources in species sorting (Sec.SI.2). In addition, the unimodal pattern of this ratio along temperature gradients suggests that, at extremely high or low temperatures (Fig. 3), cells typically allocate more energy to resource exploitation (thus limiting the growth of other species) rather than (effective) self-regulation. Notably, this effective self-regulation (α_{ii}) emerges from the consumer-resource dynamics, where cells within a population compete for shared resources. Consequently, due to complete overlap in resource preferences, intra-species competition is always stronger than inter-species competition (Fig. 2).

An additional interesting finding of our study is that the (effective) interaction matrix $\mathbf{A}$ is asymmetric, that there is no correlation between the elements of the upper and lower diagonal (Fig.SI.4, Eqn. 6). This is mainly because species have different resource uptake rates, and the impact of one species on another rarely equals the impact it experiences in return, particularly when cross-feeding is involved. Therefore, this result, along with the net competitiveness among species, holds without metabolic constraints (Fig.SI.6 and Fig.SI.7), as they both originated from the inherent properties of the ELV.

These properties of the interaction matrix $\mathbf{A}$ provide important implications for the feasibility and stability of communities across temperature gradients. We have shown that when resource mediation is incorporated, effective species interactions typically exhibit unimodal temperature performance curves (Fig. 4), and the variation of interactions is relatively lower at intermediate temperatures (Fig. 2). This aligns with the parameterization in Clegg & Pawar (2024), which identified interaction variation as a key driver of species richness along temperature gradients, predicting a unimodal richness pattern that peaks at intermediate temperatures. Previous studies also suggest that communities tend to be more stable towards environmental perturbations when interspecific interactions are weakly competitive and positive interactions are rare (Coyte et al. 2015, Butler & O'Dwyer 2018). In line with this, our results suggest that microbial communities are predominantly stable, as their effective interactions tend to be

net competitive. Moreover, since interspecific interactions vary unimodally with temperature relative to intraspecific interactions (Fig. 3), and reach a minimum at intermediate temperatures, it is plausible that the resulting community (Jacobian) matrices are more diagonally dominant at these intermediate temperatures (Haydon 1994), implying greater stability. Further mathematical and empirical analyses are required to specifically test these hypotheses, and our framework offers a promising basis for further exploration of how community feasibility and stability respond to temperature changes.

Our version of the microbial consumer resource model (MiCRM) makes two key assumptions: First, microbial species in natural environments consume and deplete surrounding resources sufficiently fast. Therefore, we assume the external supply rate of all resource types is constant where the outflow of resources is negligible, and species' resource uptake linearly correlates with resource abundance. Second, the system is well-mixed. Therefore, species have equal access to all resources without a spatial structure. While applying our framework to more specific cases, such as specific experimental environments or focal groups of species, different types of external resource input functions ($\rho_a(R_a)$; Eqn. 2) could be considered. For example, for species feeding solely on self-renewing resource $\rho_a = \frac{r_a R_a}{K_a}(K_a - R_a)$ (MacArthur 1969), the growth rate (r_a) and carrying capacity (K_a) of the self-growing resource need to be included. And for the chemostat experimental environment (Tilman 1982, Marsland III et al. 2019), $\rho_a = \chi_a(K_a - R_a)$, where χ_a is the dilution rate of resource in the system. In addition, for species growing in resource-rich media where resources are highly abundant in the environment, the Monod equation could be added to species' uptake rate, where $u = u_{max} \cdot \frac{R}{k_R + R}$, here u_{max} is the maximum uptake rate and k_R is the half saturation constant of resources.

In this work, we have assumed that the species interaction network is fully connected because all populations are able to access all resources in a well-mixed environment, with uptake preferences uniformly generated across all resource types. Also, set the leakage (substrate-metabolite transformation) fraction to be 0.3 for every species. Sec.SI.9 shows that changing leakage levels (Fig.SI.9), or the uptake structure (Sec.SI.8, Fig.SI.8; scenarios of high niche differentiation), do not qualitatively affect our results.

For more realistic predictions of community dynamics, Genome Scale Metabolic Models (GEMs) (Wang 2017) could be used to 1) map the underlying biochemical networks and enzyme kinetics of cellular-level metabolism to provide parameterisations for the leakage tensor and resource uptake matrices; 2) provide a mechanistic understanding of competitive and facilitative interactions through metabolic pathways and flux exchanges (Zelezniak et al. 2015, Machado et al. 2021). In addition, as already stated in the methods section, we are currently using the distribution of activation energies of species' r_{max}s as a proxy in parameterising resource uptake rates, while empirical measurements of the TPCs of species' uptake rates is recommended for future studies applying this framework.

Previous studies investigating the impacts of temperature on community dynamics based on consumer-resource theories focused on species interactions across trophic levels, mainly on interactions between predators (as consumers) and living resources (e.g., prey) in food webs (Kaur & Dutta 2020, Uszko et al. 2017, Amarasekare 2015). In this study, we focus on the temperature dependence of resource-mediated microbial interactions at the same trophic level, and show that species interactions are determined by the complex interplay of resource uptake and transformation. Other types of interactions are also potentially important for the dynamics of microbial communities, including predation (Pérez et al. 2016), quorum sensing (Miller & Bassler 2001, Whitehead et al. 2001), horizontal gene transfer (Arnold et al. 2022), cannibalism (González-Pastor et al. 2003), and chemical inhibition. For specific microbial communities such as phytoplankton and fungi, light competition (Huisman et al. 1999), sporulation, and other nutrients (e.g., nitrogen, phosphorus) (Koide et al. 2005) are also essential for consideration.

Future studies focusing on specific functional groups of microbes could consider extending our method to include these fundamental types of interactions of focal communities. The calculation of the feasible systems in more complex scenarios may not always be possible analytically but can be incorporated numerically into our framework.

Our framework also provides implications for empirical studies on species' interactions within natural microbial communities. Current empirical approaches available for quantitatively studying species interactions, such as counting colonies on plates (Friedman et al. 2017) is limited to simple communities composed of a few species and are hard to extend to large communities, especially when colony morphologies become hard to identify by observation. Additionally, fitting community structure snapshots to LV models requires frequent sequencing aligned with the timescale of community dynamics, which is both arduous and costly. With our framework, we demonstrate that species interactions can be quantitatively predicted from species' intrinsic metabolic properties.

In conclusion, using these consumer-resource dynamics with metabolic constraints, we provide a framework for extending the metabolic theory of ecology beyond species-level metabolic traits to ecological phenomena. Preliminarily applying our framework, we obtained three key insights. First, species' effective interactions respond unimodally to environmental temperature and exhibit higher thermal sensitivity relative to their underlying metabolic traits. Second, the temperature response of species interactions is primarily driven by competition for limited resources. Third, with increasing temperature, the strengths of intraspecific interactions increase faster than interspecific interactions.

This method we have developed and its application to bacterial systems provide the basis for inferring, estimating, or predicting the temperature-dependence of effective, pairwise microbial species interactions in a wide range of contexts and applications. In addition, our results provide new insights into the understanding of microbial species interactions and pave the way for further studies on the impacts of temperature perturbations (e.g., global warming) on the feasibility, stability, and reactivity of natural microbial communities.

5 Code Availability

Code for simulation and analysis in this study is available at https://github.com/DaniDuan/temp_interactions.git.

References

Amarasekare, P. (2015), 'Effects of temperature on consumer–resource interactions', *Journal of Animal Ecology* **84**(3), 665–679.

Andersen, K. H., Berge, T., Gonçalves, R. J., Hartvig, M., Heuschele, J., Hylander, S., Jacobsen, N. S., Lindemann, C., Martens, E. A., Neuheimer, A. B. et al. (2016), 'Characteristic sizes of life in the oceans, from bacteria to whales', *Annual review of marine science* **8**(1), 217–241.

Angilletta Jr, M. J. & Angilletta, M. J. (2009), 'Thermal adaptation: a theoretical and empirical synthesis'.

Angilletta Jr, M. J., Niewiarowski, P. H. & Navas, C. A. (2002), 'The evolution of thermal physiology in ectotherms', *Journal of thermal Biology* **27**(4), 249–268.

Arnold, B. J., Huang, I.-T. & Hanage, W. P. (2022), 'Horizontal gene transfer and adaptive evolution in bacteria', *Nature Reviews Microbiology* **20**(4), 206–218.

Bar-On, Y. M., Phillips, R. & Milo, R. (2018), 'The biomass distribution on earth', *Proceedings of the National Academy of Sciences* **115**(25), 6506–6511.

Barabás, G., Michalska-Smith, M. J. & Allesina, S. (2017), 'Self-regulation and the stability of large ecological networks', *Nature ecology & evolution* **1**(12), 1870–1875.

Barabás, G., Pásztor, L., Meszéna, G. & Ostling, A. (2014), 'Sensitivity analysis of coexistence in ecological communities: theory and application', *Ecology Letters* **17**(12), 1479–1494.

Barberán, A., Bates, S. T., Casamayor, E. O. & Fierer, N. (2012), 'Using network analysis to explore co-occurrence patterns in soil microbial communities', *The ISME journal* **6**(2), 343–351.

Bestion, E., García-Carreras, B., Schaum, C.-E., Pawar, S. & Yvon-Durocher, G. (2018), 'Metabolic traits predict the effects of warming on phytoplankton competition', *Ecology Letters* **21**(5), 655–664.

Bezanson, J., Edelman, A., Karpinski, S. & Shah, V. B. (2017), 'Julia: A fresh approach to numerical computing', *SIAM Review* **59**(1), 65–98.
URL: *https://epubs.siam.org/doi/10.1137/141000671*

Blanchet, F. G., Cazelles, K. & Gravel, D. (2020), 'Co-occurrence is not evidence of ecological interactions', *Ecology Letters* **23**(7), 1050–1063.

Butler, S. & O'Dwyer, J. P. (2018), 'Stability criteria for complex microbial communities', *Nature communications* **9**(1), 2970.

Cazelles, K., Araújo, M. B., Mouquet, N. & Gravel, D. (2016), 'A theory for species co-occurrence in interaction networks', *Theoretical Ecology* **9**, 39–48.

Chesson, P. (2000), 'Mechanisms of maintenance of species diversity', *Annual review of Ecology and Systematics* **31**(1), 343–366.

Clegg, T. & Pawar, S. (2024), 'Variation in thermal physiology can drive the temperature-dependence of microbial community richness', *eLife* **13**, e84662.
URL: *https://doi.org/10.7554/eLife.84662*

Corkrey, R., Olley, J., Ratkowsky, D., McMeekin, T. & Ross, T. (2012), 'Universality of thermodynamic constants governing biological growth rates', *PLoS One* **7**(2), e32003.

Coyte, K. Z., Schluter, J. & Foster, K. R. (2015), 'The ecology of the microbiome: networks, competition, and stability', *Science* **350**(6261), 663–666.

Dell, A. I., Pawar, S. & Savage, V. M. (2014), 'Temperature dependence of trophic interactions are driven by asymmetry of species responses and foraging strategy', *Journal of Animal Ecology* **83**(1), 70–84.

DeLong, J. P., Gibert, J. P., Luhring, T. M., Bachman, G., Reed, B., Neyer, A. & Montooth, K. (2017), 'The combined effects of reactant kinetics and enzyme stability explain the temperature dependence of metabolic rates', *Ecology and Evolution* **7**(11), 3940–3950.

DeLong, J. P., Okie, J. G., Moses, M. E., Sibly, R. M. & Brown, J. H. (2010), 'Shifts in metabolic scaling, production, and efficiency across major evolutionary transitions of life', *Proceedings of the National Academy of Sciences* **107**(29), 12941–12945.

Friedman, J., Higgins, L. M. & Gore, J. (2017), 'Community structure follows simple assembly rules in microbial microcosms', *Nature ecology & evolution* **1**(5), 0109.

García, F. C., Clegg, T., O'Neill, D. B., Warfield, R., Pawar, S. & Yvon-Durocher, G. (2023), 'The temperature dependence of microbial community respiration is amplified by changes in species interactions', *Nature microbiology* **8**(2), 272–283.

Gibson, B., Wilson, D. J., Feil, E. & Eyre-Walker, A. (2018), 'The distribution of bacterial doubling times in the wild', *Proceedings of the Royal Society B* **285**(1880), 20180789.

Gilbert, B., Tunney, T. D., McCann, K. S., DeLong, J. P., Vasseur, D. A., Savage, V., Shurin, J. B., Dell, A. I., Barton, B. T., Harley, C. D. et al. (2014), 'A bioenergetic framework for the temperature dependence of trophic interactions', *Ecology letters* **17**(8), 902–914.

Gilchrist, G. W. (1995), 'Specialists and generalists in changing environments. i. fitness landscapes of thermal sensitivity', *The American Naturalist* **146**(2), 252–270.

Gillooly, J. F., Brown, J. H., West, G. B., Savage, V. M. & Charnov, E. L. (2001), 'Effects of size and temperature on metabolic rate', *science* **293**(5538), 2248–2251.

Goldford, J. E., Lu, N., Bajić, D., Estrela, S., Tikhonov, M., Sanchez-Gorostiaga, A., Segrè, D., Mehta, P. & Sanchez, A. (2018), 'Emergent simplicity in microbial community assembly', *Science* **361**(6401), 469–474.

González-Pastor, J. E., Hobbs, E. C. & Losick, R. (2003), 'Cannibalism by sporulating bacteria', *Science* **301**(5632), 510–513.

Handley, K. M. (2019), 'Determining microbial roles in ecosystem function: redefining microbial food webs and transcending kingdom barriers', *Msystems* **4**(3), e00153–19.

Haydon, D. (1994), 'Pivotal assumptions determining the relationship between stability and complexity: an analytical synthesis of the stability-complexity debate', *The American Naturalist* **144**(1), 14–29.

Hein, Y. & Jafarpour, F. (2024), 'Asymptotic decoupling of population growth rate and cell size distribution', *Physical Review Research* **6**(4), 043006.

Hobbs, J. K., Jiao, W., Easter, A. D., Parker, E. J., Schipper, L. A. & Arcus, V. L. (2013), 'Change in heat capacity for enzyme catalysis determines temperature dependence of enzyme catalyzed rates', *ACS chemical biology* **8**(11), 2388–2393.

Huey, R. B. & Hertz, P. E. (1984), 'Is a jack-of-all-temperatures a master of none?', *Evolution* pp. 441–444.

Huisman, J., Jonker, R. R., Zonneveld, C. & Weissing, F. J. (1999), 'Competition for light between phytoplankton species: experimental tests of mechanistic theory', *Ecology* **80**(1), 211–222.

Jafarpour, F. (2019), 'Cell size regulation induces sustained oscillations in the population growth rate', *Physical Review Letters* **122**(11), 118101.

Jafarpour, F., Wright, C. S., Gudjonson, H., Riebling, J., Dawson, E., Lo, K., Fiebig, A., Crosson, S., Dinner, A. R. & Iyer-Biswas, S. (2018), 'Bridging the timescales of single-cell and population dynamics', *Physical Review X* **8**(2), 021007.

Karger, D. N., Conrad, O., Böhner, J., Kawohl, T., Kreft, H., Soria-Auza, R. W., Zimmermann, N. E., Linder, H. P. & Kessler, M. (2017), 'Climatologies at high resolution for the earth's land surface areas', *Scientific data* **4**(1), 1–20.

Kaur, T. & Dutta, P. S. (2020), 'Persistence and stability of interacting species in response to climate warming: the role of trophic structure', *Theoretical Ecology* **13**(3), 333–348.

Kehe, J., Ortiz, A., Kulesa, A., Gore, J., Blainey, P. C. & Friedman, J. (2021), 'Positive interactions are common among culturable bacteria', *Science advances* **7**(45), eabi7159.

Kempes, C. P., Dutkiewicz, S. & Follows, M. J. (2012), 'Growth, metabolic partitioning, and the size of microorganisms', *Proceedings of the National Academy of Sciences* **109**(2), 495–500.

Kempes, C. P., van Bodegom, P. M., Wolpert, D., Libby, E., Amend, J. & Hoehler, T. (2017), 'Drivers of bacterial maintenance and minimal energy requirements', *Frontiers in microbiology* **8**, 31.

Ketola, T. & Saarinen, K. (2015), 'Experimental evolution in fluctuating environments: tolerance measurements at constant temperatures incorrectly predict the ability to tolerate fluctuating temperatures', *Journal of Evolutionary Biology* **28**(4), 800–806.

Koide, R. T., Xu, B., Sharda, J., Lekberg, Y. & Ostiguy, N. (2005), 'Evidence of species interactions within an ectomycorrhizal fungal community', *New Phytologist* pp. 305–316.

Kontopoulos, D.-G., van Sebille, E., Lange, M., Yvon-Durocher, G., Barraclough, T. G. & Pawar, S. (2020), 'Phytoplankton thermal responses adapt in the absence of hard thermodynamic constraints', *Evolution* **74**(4), 775–790.

Kontopoulos, D., Smith, T. P., Barraclough, T. G. & Pawar, S. (2020), 'Adaptive evolution shapes the present-day distribution of the thermal sensitivity of population growth rate', *PLoS biology* **18**(10), e3000894.

Lechón-Alonso, P., Clegg, T., Cook, J., Smith, T. P. & Pawar, S. (2021), 'The role of competition versus cooperation in microbial community coalescence', *PLOS Computational Biology* **17**(11), e1009584.

Lee, H., Bloxham, B. & Gore, J. (2023), 'Resource competition can explain simplicity in microbial community assembly', *Proceedings of the National Academy of Sciences* **120**(35), e2212113120.

MacArthur, R. (1970), 'Species packing and competitive equilibrium for many species', *Theoretical population biology* **1**(1), 1–11.

MacArthur, R. M. (1969), 'Species packing, and what competition minimizes', *Proceedings of the National Academy of Sciences* **64**(4), 1369–1371.

Machado, D., Maistrenko, O. M., Andrejev, S., Kim, Y., Bork, P., Patil, K. R. & Patil, K. R. (2021), 'Polarization of microbial communities between competitive and cooperative metabolism', *Nature ecology & evolution* **5**(2), 195–203.

Malik, A. A., Martiny, J. B., Brodie, E. L., Martiny, A. C., Treseder, K. K. & Allison, S. D. (2020), 'Defining trait-based microbial strategies with consequences for soil carbon cycling under climate change', *The ISME journal* **14**(1), 1–9.

Marsland III, R., Cui, W., Goldford, J., Sanchez, A., Korolev, K. & Mehta, P. (2019), 'Available energy fluxes drive a transition in the diversity, stability, and functional structure of microbial communities', *PLoS computational biology* **15**(2), e1006793.

Marsland III, R., Cui, W. & Mehta, P. (2020), 'The minimum environmental perturbation principle: A new perspective on niche theory', *The American Naturalist* **196**(3), 291–305.

Marsland, R., Cui, W. & Mehta, P. (2020), 'A minimal model for microbial biodiversity can reproduce experimentally observed ecological patterns', *Scientific reports* **10**(1), 1–17.

Miller, M. B. & Bassler, B. L. (2001), 'Quorum sensing in bacteria', *Annual Reviews in Microbiology* **55**(1), 165–199.

Mongold, J. A., Bennett, A. F. & Lenski, R. E. (1996), 'Evolutionary adaptation to temperature. iv. adaptation of escherichia coli at a niche boundary', *Evolution* **50**(1), 35–43.

Morris, J. J. (2015), 'Black queen evolution: the role of leakiness in structuring microbial communities', *Trends in Genetics* **31**(8), 475–482.

Morris, J. J., Lenski, R. E. & Zinser, E. R. (2012), 'The black queen hypothesis: evolution of dependencies through adaptive gene loss', *MBio* **3**(2), e00036–12.

NOAA, N. (2024), 'Monthly global climate report for annual 2023'.
URL: *https://www.ncei.noaa.gov/access/monitoring/monthly-report/global/202313*

Padfield, D., O'Sullivan, H. & Pawar, S. (2021), 'rtpc and nls. multstart: a new pipeline to fit thermal performance curves in r', *Methods in Ecology and Evolution* **12**(6), 1138–1143.

Pascual-García, A., Bonhoeffer, S. & Bell, T. (2020), 'Metabolically cohesive microbial consortia and ecosystem functioning', *Philosophical Transactions of the Royal Society B* **375**(1798), 20190245.

Pérez, J., Moraleda-Muñoz, A., Marcos-Torres, F. J. & Muñoz-Dorado, J. (2016), 'Bacterial predation: 75 years and counting!', *Environmental Microbiology* **18**(3), 766–779.

Philippot, L., Spor, A., Hénault, C., Bru, D., Bizouard, F., Jones, C. M., Sarr, A. & Maron, P.-A. (2013), 'Loss in microbial diversity affects nitrogen cycling in soil', *The ISME journal* **7**(8), 1609–1619.

Pold, G., Domeignoz-Horta, L. A., Morrison, E. W., Frey, S. D., Sistla, S. A. & DeAngelis, K. M. (2020), 'Carbon use efficiency and its temperature sensitivity covary in soil bacteria', *MBio* **11**(1), 10–1128.

Rivett, D. W. & Bell, T. (2018), 'Abundance determines the functional role of bacterial phylotypes in complex communities', *Nature microbiology* **3**(7), 767–772.

Schoolfield, R. M., Sharpe, P. & Magnuson, C. E. (1981), 'Non-linear regression of biological temperature-dependent rate models based on absolute reaction-rate theory', *Journal of theoretical biology* **88**(4), 719–731.

Smith, T. P., Clegg, T., Bell, T. & Pawar, S. (2021), 'Systematic variation in the temperature dependence of bacterial carbon use efficiency', *Ecology Letters* **24**(10), 2123–2133.

Smith, T. P., Thomas, T. J., García-Carreras, B., Sal, S., Yvon-Durocher, G., Bell, T. & Pawar, S. (2019), 'Community-level respiration of prokaryotic microbes may rise with global warming', *Nature communications* **10**(1), 5124.

Stark, K. A., Clegg, T., Bernhardt, J. R., Grainger, T. N., Kempes, C. P., Savage, V., O'Connor, M. I. & Pawar, S. (2024), 'Towards a more dynamic metabolic theory of ecology to predict climate change effects on biological systems'.

The Human Microbiome Project Consortium, Huttenhower, C., Gevers, D., Knight, R., Abubucker, S., Badger, J. H., Chinwalla, A. T., Creasy, H. H., Earl, A. M., Fitzgerald, M. G., Fulton, R. S., Giglio, M. G., Hallsworth-Pepin, K., Lobos, E. A., Madupu, R., Magrini, V., Martin, J. C., Mitreva, M., Muzny, D. M., Sodergren, E. J., Versalovic, J., Wollam, A. M., Worley, K. C., Wortman, J. R., Young, S. K., Zeng, Q., Aagaard, K. M., Abolude, O. O., Allen-Vercoe, E., Alm, E. J., Alvarado, L., Andersen, G. L., Anderson, S., Appelbaum, E., Arachchi, H. M., Armitage, G., Arze, C. A., Ayvaz, T., Baker, C. C., Begg, L., Belachew, T., Bhonagiri, V., Bihan, M., Blaser, M. J., Bloom, T., Bonazzi, V., Paul Brooks, J., Buck, G. A., Buhay, C. J., Busam, D. A., Campbell, J. L., Canon, S. R., Cantarel, B. L., Chain, P. S. G., Chen, I. M. A., Chen, L., Chhibba, S., Chu, K., Ciulla, D. M., Clemente, J. C., Clifton, S. W., Conlan, S., Crabtree, J., Cutting, M. A., Davidovics, N. J., Davis, C. C., Desantis, T. Z., Deal, C., Delehaunty, K. D., Dewhirst, F. E., Deych, E., Ding, Y., Dooling, D. J., Dugan, S. P., Michael Dunne, W., Scott Durkin, A., Edgar, R. C., Erlich, R. L., Farmer, C. N., Farrell, R. M., Faust, K., Feldgarden, M., Felix, V. M., Fisher, S., Fodor, A. A., Forney, L. J., Foster, L., di Francesco, V., Friedman, J., Friedrich, D. C., Fronick, C. C., Fulton, L. L., Gao, H., Garcia, N., Giannoukos, G., Giblin, C., Giovanni, M. Y., Goldberg, J. M., Goll, J., Gonzalez, A., Griggs, A., Gujja, S., Kinder Haake, S., Haas, B. J., Hamilton, H. A., Harris, E. L., Hepburn, T. A., Herter, B., Hoffmann, D. E., Holder, M. E., Howarth, C., Huang, K. H., Huse, S. M., Izard, J., Jansson, J. K., Jiang, H., Jordan, C., Joshi, V., Katancik, J. A., Keitel, W. A., Kelley, S. T., Kells, C., King, N. B., Knights, D., Kong, H. H., Koren, O., Koren, S., Kota, K. C., Kovar, C. L., Kyrpides, N. C., La Rosa, P. S., Lee, S. L., Lemon, K. P., Lennon, N., Lewis, C. M., Lewis, L., Ley, R. E., Li, K., Liolios, K., Liu, B., Liu, Y., Lo, C.-C., Lozupone, C. A., Dwayne Lunsford, R., Madden, T., Mahurkar, A. A., Mannon, P. J., Mardis, E. R., Markowitz, V. M., Mavromatis, K., McCorrison, J. M., McDonald, D., McEwen, J., McGuire, A. L., McInnes, P., Mehta, T., Mihindukulasuriya, K. A., Miller, J. R., Minx, P. J., Newsham, I., Nusbaum, C., O'Laughlin, M., Orvis, J., Pagani, I., Palaniappan, K., Patel, S. M., Pearson, M., Peterson, J., Podar, M., Pohl, C., Pollard, K. S., Pop, M., Priest, M. E., Proctor, L. M., Qin, X., Raes, J., Ravel, J., Reid, J. G., Rho, M., Rhodes, R., Riehle, K. P., Rivera, M. C., Rodriguez-Mueller, B., Rogers, Y.-H., Ross, M. C., Russ, C., Sanka, R. K., Sankar, P., Fah Sathirapongsasuti, J., Schloss, J. A., Schloss, P. D., Schmidt, T. M., Scholz, M., Schriml, L., Schubert, A. M., Segata, N., Segre, J. A., Shannon, W. D., Sharp, R. R., Sharpton, T. J., Shenoy, N., Sheth, N. U., Simone, G. A., Singh, I., Smillie, C. S., Sobel, J. D., Sommer, D. D., Spicer, P., Sutton, G. G., Sykes, S. M., Tabbaa, D. G., Thiagarajan, M., Tomlinson, C. M., Torralba, M., Treangen, T. J., Truty, R. M., Vishnivetskaya, T. A., Walker, J., Wang, L., Wang, Z., Ward, D. V., Warren, W., Watson, M. A., Wellington, C., Wetterstrand, K. A., White, J. R., Wilczek-Boney, K., Wu, Y., Wylie, K. M., Wylie, T., Yandava, C., Ye, L., Ye, Y., Yooseph, S., Youmans, B. P., Zhang, L., Zhou, Y., Zhu, Y., Zoloth, L., Zucker, J. D., Birren, B. W., Gibbs, R. A., Highlander, S. K., Methé, B. A., Nelson, K. E., Petrosino, J. F., Weinstock, G. M., Wilson, R. K. & White, O. (2012), 'Structure, function and diversity of the healthy human microbiome', **486**(7402), 207–214.

Thompson, L. R., Sanders, J. G., McDonald, D., Amir, A., Ladau, J., Locey, K. J., Prill, R. J., Tripathi, A., Gibbons, S. M., Ackermann, G. et al. (2017), 'A communal catalogue reveals earth's multiscale microbial diversity', *Nature* **551**(7681), 457–463.

Tikhonov, M. (2016), 'Community-level cohesion without cooperation', *Elife* **5**, e15747.

Tilman, D. (1982), *Resource competition and community structure*, number 17, Princeton university press.

Uszko, W., Diehl, S., Englund, G. & Amarasekare, P. (2017), 'Effects of warming on predator–prey interactions–a resource-based approach and a theoretical synthesis', *Ecology Letters* **20**(4), 513–523.

Wang, D. (2017), 'Systems biology: Constraint-based reconstruction and analysis'.

West, G. B., Brown, J. H. & Enquist, B. J. (1997), 'A general model for the origin of allometric scaling laws in biology', *Science* **276**(5309), 122–126.

Whitehead, N. A., Barnard, A. M., Slater, H., Simpson, N. J. & Salmond, G. P. (2001), 'Quorum-sensing in gram-negative bacteria', *FEMS microbiology reviews* **25**(4), 365–404.

Woolway, R. I., Jones, I. D., Maberly, S. C., French, J. R., Livingstone, D. M., Monteith, D. T., Simpson, G. L., Thackeray, S. J., Andersen, M. R., Battarbee, R. W. et al. (2016), 'Diel surface temperature range scales with lake size', *Plos one* **11**(3), e0152466.

Zelezniak, A., Andrejev, S., Ponomarova, O., Mende, D. R., Bork, P. & Patil, K. R. (2015), 'Metabolic dependencies drive species co-occurrence in diverse microbial communities', *Proceedings of the National Academy of Sciences* **112**(20), 6449–6454.